Mechanisms Governing 90Sr Removal and Remobilisation in a VLLW Surface Disposal Concept

Ho, Mallory S.

Multidisciplinary Digital Publishing Institute
2023-03-18

Ho, M.S.; Vettese, G.F.; Keto, P.H.; Lamminmäki, S.P.; Vikman, M.; Myllykylä, E.; Dardenne, K.; Law, G.T.W. Mechanisms Governing 90Sr Removal and Remobilisation in a VLLW Surface Disposal Concept. Minerals 2023, 13, 436.

http://hdl.handle.net/10138/356610

minerals

MDPI

Article

Mechanisms Governing ^{90}Sr Removal and Remobilisation in a VLLW Surface Disposal Concept

Mallory S. Ho [1], Gianni F. Vettese [1,*], Paula H. Keto [2], Suvi P. Lamminmäki [2], Minna Vikman [2], Emmi Myllykylä [2], Kathy Dardenne [3] and Gareth T. W. Law [1,*]

[1] Radiochemistry Unit, The University of Helsinki, FI-00014 Helsinki, Finland
[2] VTT Technical Research Centre of Finland, FI-02044 Espoo, Finland
[3] Institute for Nuclear Waste Disposal, Karlsruhe Institute of Technology, 76344 Eggenstein-Leopoldshafen, Germany
* Correspondence: gianni.vettese@helsinki.fi (G.F.V.); gareth.law@helsinki.fi (G.T.W.L.)

Abstract: Flow-through columns were used to assess potential long-term trends in ^{90}Sr biogeochemistry and transport in a Finnish near-surface very low-level waste (VLLW) repository concept. Experiments simulated the effects of water intrusion and flow through the repository barrier and backfill materials, examining impacts on ^{90}Sr migration. Artificial rainwater containing 2.0 mg/L stable Sr (as a proxy for ^{90}Sr) was pumped through column systems that had varying compositions from a matrix of rock flour (backfill material), bentonite (backfill/sealing material), and carbon steel (waste encapsulation material), for 295 days. Effluent geochemistry was monitored throughout. Sr retention behaviour in all column systems was broadly similar. Sr removal from influent rainwater was marked (~95% removed) at the beginning of the experiments, and this degree of removal was maintained for 20 days. Thereafter, Sr concentrations in the effluents began to rise, reaching ~2 mg/L by 295 days. Further, 56%–67% of added Sr was retained in the repository materials over the 295-day reaction period. Analysis of the effluents indicated that colloids did not form; as such, Sr output was likely to be aqueous Sr^{2+}. Upon completion of the experiment, solid-associated Sr distribution and speciation in the columns were assessed through column sectioning and post-mortem analyses, which encompassed the following: total acid digests, sequential extractions, and XAS analysis. The total acid digests and sequential extractions showed that Sr was evenly distributed throughout the columns and that the majority (68%–87%) of solid-associated Sr was in the exchangeable fraction ($MgCl_2$). This suggested that a major part of the solid-phase Sr was weakly bound to the column materials via outer-sphere sorption. Interestingly, a smaller amount of Sr (7%–23%) could only be extracted by aqua regia, suggesting that a proportion of Sr may bind more strongly to the barrier materials. XAS analysis of select samples confirmed that the dominant Sr phase was sorbed to the rock flour and bentonite, but not corroded carbon steel. Columns were also subject to remobilisation experiments using artificial rain- and seawater without added Sr. While rainwater remobilised Sr slowly, high-ionic strength seawater remobilised Sr at much higher rates in the systems containing bentonite. Interestingly, Sr was well retained in the rock flour-only system following rain and seawater intrusion. Overall, the results indicate that the column materials provide reactive surfaces for Sr removal should it be released from waste packages; however, the backfill and barrier materials have limited retention capacity, and the dominant sorption interaction is relatively weak. The safety case for the shallow disposal of radioactive waste should consider the possibility of seawater intrusion and that the bentonite-bound Sr was significantly more susceptible to remobilisation following seawater, despite retaining slightly more Sr during sorption experiments.

Keywords: very low-level radioactive waste disposal; strontium; bentonite; flow-through columns; EXAFS

Citation: Ho, M.S.; Vettese, G.F.; Keto, P.H.; Lamminmäki, S.P.; Vikman, M.; Myllykylä, E.; Dardenne, K.; Law, G.T.W. Mechanisms Governing ^{90}Sr Removal and Remobilisation in a VLLW Surface Disposal Concept. *Minerals* **2023**, *13*, 436. https://doi.org/10.3390/min13030436

Academic Editors: Katharina Müller and Norbert Jordan

Received: 3 January 2023
Revised: 7 March 2023
Accepted: 10 March 2023
Published: 18 March 2023

1. Introduction

The near-surface disposal of very low-level radioactive wastes (VLLWs), containing radionuclides with half-lives less than ~30 years, is an attractive waste management option that will be/is employed by many countries, including Finland, Sweden, and the UK [1–3]. Here, given the short half-lives of the radionuclides, the burial concept is only required to contain/isolate the radionuclides from the surrounding biosphere for several hundred years [4]. VLLW repositories use a multi-barrier concept comprising several independent engineered barriers (waste matrix, waste container, buffer, and backfill), as well as a natural host rock/geological barrier that will ensure the long-term stewardship of the radioactive waste [4]. Ultimately, any radionuclides that are released from the waste packages will be diluted and their mobility should be significantly impeded by the barriers before they cause any radiological or toxicity impacts in the biosphere.

Currently, Finnish VLLW is disposed of in underground repositories (60–100 m depth; known as the VLJ-caves) that were originally designed for low- and intermediate-level waste (LILW) disposal [3]. Some Finnish VLLW has also been stored in special landfills [5]; however, due to limitations set in the EU landfill directive (1999/31/EC of April 1999 updated with 2018/850/EC) concerning the disposal of organic wastes in landfills, the renewal of these licences is no longer a valid option for the future. The Finnish Nuclear Energy Act (990/1987) permits the storage of VLLW in near-surface repositories [6]. Implementation of this waste management approach for VLLW would permit fuller use of existing VLJ-caves for LILW disposal, offering significant cost savings as VLLW is voluminous and new-build LILW could instead be placed in the VLJ-caves [3].

The Finnish utility Teollisuuden Voima Oyj (TVO) is currently in the advanced stages of planning a near-surface disposal facility at the Olkiluoto nuclear power plant, which is located on the Gulf of Bothnia coast. TVO operates the Olkiluoto site, and they are responsible for the management of wastes generated from site activities. They have completed two environmental impact assessments in 2020 and 2021 [7,8] that will be considered by the Finnish nuclear regulator STUK, alongside a safety case. If the safety of the approach is adequately demonstrated, the facility should be constructed and commence operations in the 2020s. It will be designed to operate for ~70 years [7,8]. During the lifetime of the near-surface repository, water intrusion to the waste packages could eventually cause radionuclide release into the surrounding environment (through the engineered and natural barriers, and ultimately into the biosphere). Here, radionuclide migration will be affected by multiple factors, including interactions with the waste packages, barrier materials, and backfill via sorption and precipitation reactions, ion-exchange, and colloid formation. Radionuclide transport will also be affected by microbial activity, e.g., the biodegradation of organic operational wastes, which can result in the creation of complexing ligands (e.g., [9]).

The near-surface repository at Olkiluoto will largely resemble a special landfill for hazardous waste [7,8] (Supplementary Materials Figure S1). Depending on the waste form, the radioactive waste will be compressed into pallets or stored in containers fabricated from carbon steel, providing mechanical and structural stability to the waste packages until the steel corrodes. The space between the waste packages may be backfilled with rock flour or crushed rock providing both a drainage function and some sorption capacity. A mineral sealing layer consisting of crushed rock and a relatively small proportion of bentonite (~6 wt.%) will also be used in the cover and foundation structures of the repository to limit the ingress of water into the waste and eventually radionuclide release through the underlying barriers [10]. Bentonite has multiple characteristics that make it a particularly suitable sealing material. It has a low permeability, which retards water transport, and a high sorption capacity for radionuclides; it also has good E_h and pH buffering capacities and possesses excellent mechanical properties (high swelling capacity and plasticity) [11].

Despite risk assessment and safety case development, there are still uncertainties regarding the long-term performance of the individual barriers and their behaviour in unison. In particular, the Finnish near-surface repository will be exposed to extreme variations in the environment (e.g., rainfall, changes in temperature, annual freezing

and thawing of the topmost barrier layer, and possible climate change impacts, such as sea-level rise). Moreover, considering the half-lives of key risk-driving radionuclides that will be present in the repository (^{90}Sr $t_{1/2}$ = 28.8 y, ^{137}Cs $t_{1/2}$ = 30.1 y), the service life of the repository is up to 300 years [12]. During this period the repository may be subject to the intrusion of oxic waters, either as rainwater or seawater (increasing influent salinity), which may be capable of remobilising radionuclides retained in wastes or on repository materials [10,13–16]. Consequently, the long-term transport of key, risk-driving radionuclides under disposal conditions must be studied. In this work, ^{90}Sr was selected from the very low-level radioactive waste inventory for further study. Specifically, we examined ^{90}Sr transport through the relevant barrier, backfill, and waste encapsulation materials (rock flour, bentonite, and steel).

^{90}Sr is a fission product in nuclear reactors. Its relatively long half-life (28.8 years), high energy β^- emission (546 keV), energetic, short-lived daughter (^{90}Y, half-life 64 h, β^- emission 2.3 MeV), and environmental mobility, make it a radionuclide of concern for the surface disposal of radioactive wastes and in contaminated land management. For example, failed storage of spent nuclear fuel has led to significant ^{90}Sr leaks globally, including at Hanford and Oak Ridge, USA [17–19]; Mayak, Russia [20], and Sellafield, UK [21]. Further, in mammals, ingested ^{90}Sr may substitute for Ca in the bones, which then irradiates bone marrow and increases the chances of contracting bone cancer or leukaemia [22].

Under moderate environmental conditions (low ionic strength, pH 4–10), ^{90}Sr is present as Sr^{2+}, which behaves similarly to Ca^{2+}. Its mobility is generally governed by sorption to sediments and minerals with a large surface area and high cation exchange capacity, e.g., clay minerals (illite, chlorite, kaolinite, and montmorillonite) [23–27] and Fe-oxides [25,28–34]. Aqueous Sr can also sorb to the charged passivating oxide layer of steel and its corrosion products [32,35,36], which are used as packaging materials during the disposal of ^{90}Sr-containing waste. Sr sorption occurs in competition with other mono and divalent cations and is thus influenced by pH, the ionic strength of the surrounding waters, and the cation-exchangeable content of mineral surfaces [25,27,37–40]. Biostimulation of aquifers via electron-donor amendments (e.g., acetate, lactate, or glycerol) have no direct effect on Sr removal from solution as it is not redox-active, but indirect mineralogical changes can marginally impact Sr mobility [23,24,41,42]. For example, the precipitation of amorphous Fe(II)-bearing biominerals, from the bioreduction of Fe(III), enhances Sr removal from solution by providing sorption sites [43]. Sr can also incorporate into Ca-carbonate minerals (e.g., calcite) [44] or Ca-phosphate (bio)minerals (e.g., hydroxyapatite), where Sr^{2+} substitutes for Ca^{2+} in the mineral lattice [23,45,46].

Sr behaviour in the environment has been extensively studied using batch microcosm experiments (see references above), which can provide useful information on removal rates and retention mechanisms, but their applicability to actual subsurface Sr transport is limited. Environmental Sr studies under more realistic conditions (e.g., column or field studies) are few. Although more complex and time-consuming, column experiments offer a much better approximation of the conditions likely to be observed in the field. Specifically, column studies (i) better reflect material packing densities and porosities that would be observed in real disposal scenarios, (ii) permit experimentation at more representative solid:solution ratios, and (iii) allow for studies with water flow at radionuclide concentrations more representative of the real world. Thorpe et al. (2017) investigated the effects of acetate amendments on Sr sorption in flow-through columns with sediment representative of the UK Sellafield site and concluded that biogeochemical perturbations involving reduction and oxidation cycles only had limited impacts on Sr retention [24]. Multiple groups have also used flowing columns to test the adequacy of simulated Sr movement via transport modelling [47–50]. The output of this work and comparison to past studies indicates that batch experiments do not yield applicable distribution coefficients to describe Sr transport in real-world scenarios.

Here, we assessed the mobility of ^{90}Sr under conditions that would prevail in the current Finnish near-surface repository concept. To understand removal rates and potential

retention mechanisms of Sr with respect to the evolving disposal facility and the effects of the engineered barrier materials and steel canister corrosion under realistic conditions, we used a flow-through column system with combinations of rock flour, bentonite (6 wt.%), carbon–steel coupons, and simulant rainwater. Sr was added to the simulant rainwater and its migration and retention in the column systems were monitored over 295 days. When Sr retention on the repository materials was observed, sequential extractions and X-ray absorption spectroscopy were used to assess the strength and mechanisms of Sr retention. Dynamic light scattering was used to ascertain if colloid-facilitated Sr transport occurred. The affinity of any solid-associated Sr towards remobilisation was also assessed in short (56 days) remobilisation studies using rainwater (28 days) and then seawater ingress (28 days) (both without added Sr). The outputs of the column experiments can be used to better parameterise the Finnish VLLW safety case.

2. Materials and Methods

2.1. Column Design and Sorption Experiments

A flow-through column system based on previous studies [51,52] was used to explore Sr behaviour under dynamic repository conditions in the worst case scenario, where the early failure of a waste package leads to radionuclide release. A schematic of the column setup can be found in the Supplementary Materials (SM) (Figure S2). Briefly, a 10 cm polypropylene column with a 1 cm inner diameter was packed tightly with the column material(s) and terminated on each end with glass wool and quartz sand. The columns were then sealed with Bola GL14 screw caps, and a peristaltic pump was used to pump simulated rainwater (Table 1) spiked with stable Sr through the columns at a constant flow rate. The rainwater recipe was based on long-term observations of rainwater compositions at the Olkiluoto nuclear power plant [53].

Table 1. Synthetic rainwater composition used in the study, adapted from [53].

Component	Rainwater (mg/L)
K_2SO_4	1.7
$CaSO_4$	2.3
$SrCl_2 \cdot 6H_2O$	6.1
NaBr	5.1
$Mg_3\ (PO_4) \cdot 6H_2O$	1.2
H_2SO_4	1.3
HNO_3	5.6
NH_4OH	3.7
pH	5.1
Ionic strength (mg/L)	24.4
Ionic strength (mM)	0.47

Three column systems with different combinations of repository materials (for a detailed characterisation see Supplementary Materials Section S3) were used in this study: (i) rock flour, (ii) rock flour + bentonite (6 wt.%), and (iii) rock flour + bentonite (6 wt.%) + carbon steel coupons (1 wt.%). The rock flour was made from locally quarried mafic igneous rock, and the bentonite was LUXGEL EG 28, which is a commercially available Ca-bentonite. In the carbon steel-containing system, ~0.1 g of 0.1 cm^3 steel coupons (mild steel EN 10130/AISI 1008) was added and positioned 1.5 cm above the column inlet. Autoclaved Sr (2.0 mg/L)-amended synthetic rainwater (pH 5, Table 1) was pumped into the base of the columns at a flowrate of 0.5 ± 0.1 mL/h. Stable Sr was added to the influent as a surrogate for ^{90}Sr and an air-bubbler was used to maintain O_2 in the influent. All column systems were reacted under ambient laboratory conditions, with constant flow for 295 days, in the dark, at 21 ± 2 °C. These conditions were chosen as a best practical representation of the expected in situ conditions. It should be noted that despite seasonal fluctuations in temperature in Finland, the interior of the Finnish near-surface repository should remain

at >0 °C during its service life (up to 300 years) [54]. Duplicate columns were run for all systems. All chemicals used were of analytical grade.

2.2. Sampling, Column Sacrifice, and Geochemical Characterisation

Under anoxic conditions (Ar flushing), effluent samples were collected at regular intervals using a syringe, as per Ho et al. (2022), and subsequent sample handling was conducted in an Ar-filled glove bag [52]. Following sampling and centrifugation (1.44×10^4 *g*, 5 min), the supernatant was monitored for physical and chemical changes. Effluent pH was measured using a calibrated electrode (Mettler-Toledo, Columbus, OH, USA) and effluent Sr concentrations ($Sr_{(aq)}$ in Figure 1 and Figure 5) were measured using inductively coupled plasma mass spectrometry (ICP-MS) (Agilent 7800, Agilent, Tokyo, Japan) from acidified (0.5% HNO_3) samples. The presence of colloids (particles with a diameter <1000 nm) in the effluent was assessed through use of dynamic light scattering (DLS) and zetapotential analysis (Zetasizer nanoZS, Malvern Panalytical Ltd., Malvern, UK).

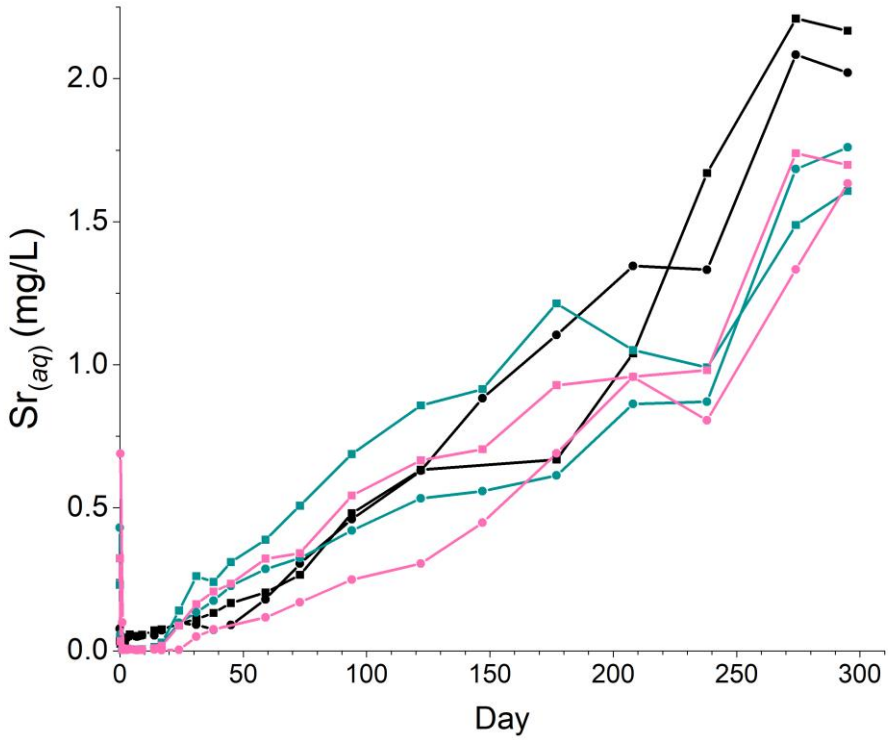

Figure 1. Concentration of $Sr_{(aq)}$ in the effluents for three column systems over 295 days: (**black**) rock flour, (**green**) rock flour + bentonite (6 wt.%), and (**pink**) rock flour + bentonite (6 wt.%) + steel coupons, after centrifugation at 1.4×10^4 *g* for 5 mins. Each system was conducted in duplicate, and individual columns (per system) are represented by squares and circles.

At the experiment end-point (295 days), one of each parallel set of columns was sliced along its length and sectioned at 0.5 cm intervals under an Ar atmosphere to study the distribution and speciation of Sr within the column material. The sections were homogenised and split for different analyses. An aliquot of each section was stored under an Ar atmosphere at −80 °C prior to X-ray absorption spectroscopy (XAS) analysis. Another aliquot was digested in boiling aqua regia for elemental analysis via ICP-MS to estimate total Sr retention along the column length. Further, the 0.5 N HCl extractable Fe(II) and total 0.5 N HCl extractable Fe content was determined in the sample sections using the ferrozine method [55]. Finally, sequential extractions (Table 2) were used to determine Sr association with different components of the disposal materials using defined chemical lixiviants adapted from relevant literature [23,56,57]. Here, ~0.1 g of sample was added to pre-weighed 15 mL centrifuge tubes and accurately weighed before adding the first

lixiviant. The lixiviants, target extraction phases, and timings are summarised in Table 2. All extraction chemicals were thoroughly sparged with Ar before use. After shaking with a rotating shaker for the required time at room temperature, solids were separated via centrifugation (1.4×10^4 *g* for 15 min), and the supernatant was collected. The residual phase was then extracted in boiling aqua regia. Supernatant samples were diluted, acidified with 0.5% HNO_3, and analysed for Sr content with ICP-MS. In between extractions, the sediment was rinsed with DI; the rinses were also monitored for Sr using ICP-MS, but they were consistently below the limit of detection. As Sr was present in the starting materials (rock flour and bentonite), the extractable Sr was determined for each step and subtracted as the background before use in the paper (Tables S1 and S2).

Table 2. Chemical lixiviants used in the sequential extraction and the respective phases targeted per step. The chemicals used in the first three steps were sparged with N_2 prior to use.

Fraction	Lixiviant	Time	Targeted Phase(s)
Exchangeable	1 M magnesium chloride (pH 7)	2 h	Sorbed
Carbonate	1 M sodium acetate (pH 5)	5 h	Carbonate minerals
Reducible	0.5 M hydroxylammonium chloride (pH 1.5)	16 h	Fe/Mn oxides
Oxidisable	30% hydrogen peroxide, 1 M ammonium acetate (pH 5)	6 h, 16 h	Organic matter
Residual	Aqua regia	4 h	Residual

2.3. X-ray Absorption Spectroscopy (XAS)

Sr speciation and local coordination was investigated using X-ray absorption near edge structure (XANES) and extended X-ray absorption fine structure (EXAFS) analysis. XAS data were collected on the Sr K-edge at the INE-Beamline at the KIT Light Source (Karlsruhe, Germany) [58], in fluorescence mode at 298 K, with two Vortex SDD detectors (ME4 and 60EX, Hitachi, Chatsworth, CA, USA) and were calibrated using the L_1-edge of a Pb metal foil (energy of the first inflexion point of the rising edge set to 15,861.0 eV). Athena was used for background subtraction, normalisation, and XANES analysis, and EXAFS spectra were fitted shell-by-shell in Artemis (Demeter) [59]. Here, F-testing was used to determine the statistical viability of additional backscattering shells [60]. The fitting procedure was constrained to fixed values for the passive electron reduction factor ($S_0{}^2$) and the Sr coordination number to determine values for the Debye−Waller factor (σ^2) and bond distances.

2.4. Remobilisation Experiments

After 295 days of flowing column experiments (as described above), one of two parallel columns was used in later remobilisation experiments to examine the stability of Sr associated with the barrier material (rock flour, bentonite, and steel) during the influx of rain- and seawater (without added Sr). Rainwater was used as a likely influent that may enter the repository due to degradation of the sealing materials over time. Brackish seawater was used as a worst-case scenario assessing the effects of potential flooding of the repository following sea-level rise due to climate change, which is a concern for LLW repositories globally [10,13–16]. Accordingly at the end of the reactions, the influent solution was amended to synthetic rainwater without added Sr. The rainwater remobilisation experiment ran for 28 days, and it was then changed to synthetic seawater representative of Baltic seawater, which ran for a further 28 days (Table 3) [61]. Throughout all experiments, an air bubbler was used to maintain oxic conditions in the influent solutions, and the flow rate (0.5 ± 0.1 mL/h) remained the same.

Table 3. Synthetic seawater composition used in the study, adapted from [61].

Component	Seawater (mg/L)
NaCl	4680
$MgCl_2$	1360
$MgSO_4 \cdot 7H_2O$	560
$CaCl_2 \cdot 2H_2O$	460
K_2SO_4	150
$CaCO_3$	20
NH_4Cl	16.1
K_2HPO_4	1.5
pH	8.1
Ionic strength (mg/L)	6057.7
Ionic strength (mM)	145.16

3. Results and Discussion

3.1. Column Effluent Geochemistry

Throughout the experiment, the column effluent geochemistry was monitored to understand the Sr concentration, speciation, and potential retention mechanisms on the backfill and barrier materials. Effluent monitoring suggested that there were no significant differences in pH (Figure S4) or $Sr_{(aq)}$ behaviour (Figure 1) among the three column systems. The effluent pH from all column systems was initially high (pH 9–10), reflecting the mafic nature of the rock flour; however, it decreased during the experiment reaching pH ~6.5 after 150 days and then slowly decreased to ~6 after 295 days (Figure S4). After an initial spike in effluent Sr that has also been observed in past experiments using this column setup [52], <10% of added Sr remained in the effluent of all systems (0.01–0.07 mg/L) during the first 20 days of the experiment (Figure 1). Subsequently, Sr concentrations in the effluent increased steadily from ~0.1 mg/L to between 1.7 and 2.2 mg/L throughout the remainder of the experiment. Here, the gradual increase in effluent Sr output was presumably due to Sr^{2+} sorption sites becoming saturated in the repository materials or due to the decrease in availability of sorption sites, linked to a drop in pH (~3 pH units) over the course of the experiment.

The effluent Sr data (Figure 1) suggest that the addition of bentonite (6 wt.%) and/or steel coupons did not significantly affect the rate or overall extent of Sr retention. Columns retained 3.9–4.7 mg of added Sr (total added Sr, 7.1 mg) and on average, duplicate columns retained 56%, 62%, and 67% of added Sr in the (i) rock flour, (ii) rock flour + bentonite, and (iii) rock flour + bentonite + carbon steel systems, respectively (Supplementary Materials Table S3). Under the basic-to-circumneutral conditions in the column systems, outer-sphere sorption of Sr^{2+} to clay and mineral surfaces (via cation exchange) present in the rock flour and bentonite was likely the dominant Sr-removal mechanism [25,28–32]. To verify this, sequential extractions and XAS analysis were performed on the column solids at the end of the experiment (295 days).

During the experiment, potential colloid formation and stability were assessed using dynamic light scattering and zeta potential measurements. Colloids can have high environmental mobility and are therefore a risk driver for enhanced radionuclide mobility from disposed wastes. Whilst bentonites offer multiple advantages as backfill materials, they are known to form colloids [62–66]. Further, bentonite colloids also have the potential to sorb radionuclides, including Sr [65–68]. Dynamic light scattering measurements for effluent samples collected on day 0 and day 220 were below the method detection limits, suggesting that significant amounts of colloids were not forming and that they were not responsible for Sr transport. This was confirmed through zeta-potential measurements, which yielded an average zeta-potential of -1.19 (± 0.242) μmcm/Vs, suggesting that no stable colloids formed. Given the ionic strength ($I = 2.4 \times 10^{-4}$ M) and pH (6–10) of the influent waters, the lack of colloids in these samples is unsurprising [69,70]. Although colloids are reported as stable in solutions with higher ionic strength, the pH of the barrier/backfill systems are

appropriately placed to be close to the point of zero charge reported for bentonite colloids (~pH 7–9) [62], thus likely promoting their aggregation and retention in the column materials, if forming. As such, the data suggest that bentonite colloids are not likely to influence radionuclide mobility in the Finnish near-surface repository concept under the timescale and conditions employed.

3.2. Solid-Phase Geochemistry

3.2.1. Acid Digests and Sequential Extractions

After 295 days of constant rainwater addition with added Sr^{2+}, the columns were sectioned into 0.5 cm horizons for solid-phase analysis. Results from the aqua regia digests demonstrated that Sr was distributed throughout each column, with concentrations in individual sections varying between ~200 and 700 µg Sr/g of solids (Figure 2A); 0.5 N HCl extractable Fe concentrations varied between 330 and 985 µg Fe/g of solids (Figure 2B). During sectioning of the rock flour + bentonite (6 wt.%) + carbon steel coupon column, a rust-coloured horizon was observed between 1.5 and 2.0 cm from the inlet, suggesting that the carbon steel coupons had corroded during the experiment. Indeed, carbon steel corrosion was expected under the experimental conditions, as documented in similar environmental systems [71,72]. Interestingly, Sr was evenly distributed throughout the columns in all systems, and the presence of steel or steel corrosion did not seem to affect Sr retention (Figure 1), consistent with previous studies [73].

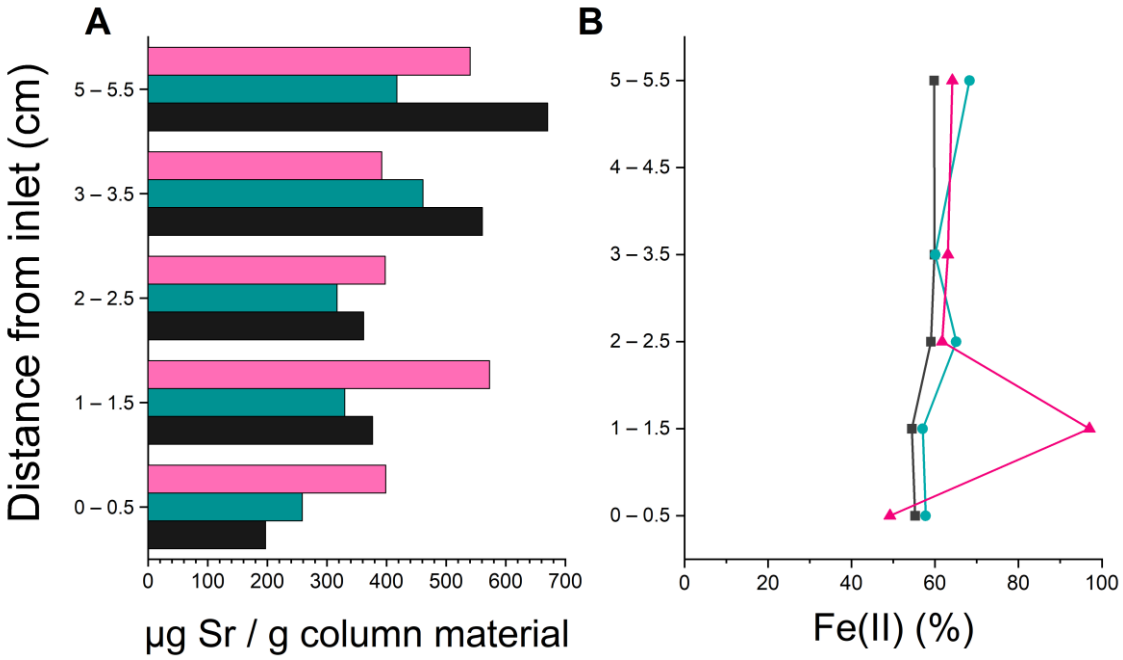

Figure 2. (**A**) Concentration of Sr and (**B**) 0.5 N HCl extractable Fe(II) expressed as a % of total 0.5 N HCl extractable Fe from selected column material samples (0.5 cm depth increments) from the three column systems: (**black squares**) rock flour, (**green circles**) rock flour + bentonite (6 wt.%), and (**pink triangles**) rock flour + bentonite (6 wt.%) + steel coupons. Sr present in starting materials was subtracted before plotting (Supplementary Materials Table S2). The steel coupons were added at a distance of 1.5 cm from the inlet.

Sequential extractions (Figure 3) showed that the majority of Sr (68%–87%) was exchangeable with 1 M $MgCl_2$, suggesting that Sr was predominantly weakly bound to the solids via outer-sphere sorption mechanisms [25,28–32]. From the remainder of extracted Sr, 7%–23% was dissolved with aqua regia, suggesting that some Sr was more strongly bound and resistant to acid remobilisation. Hence, to further probe Sr speciation in the solids, XAS analysis was used.

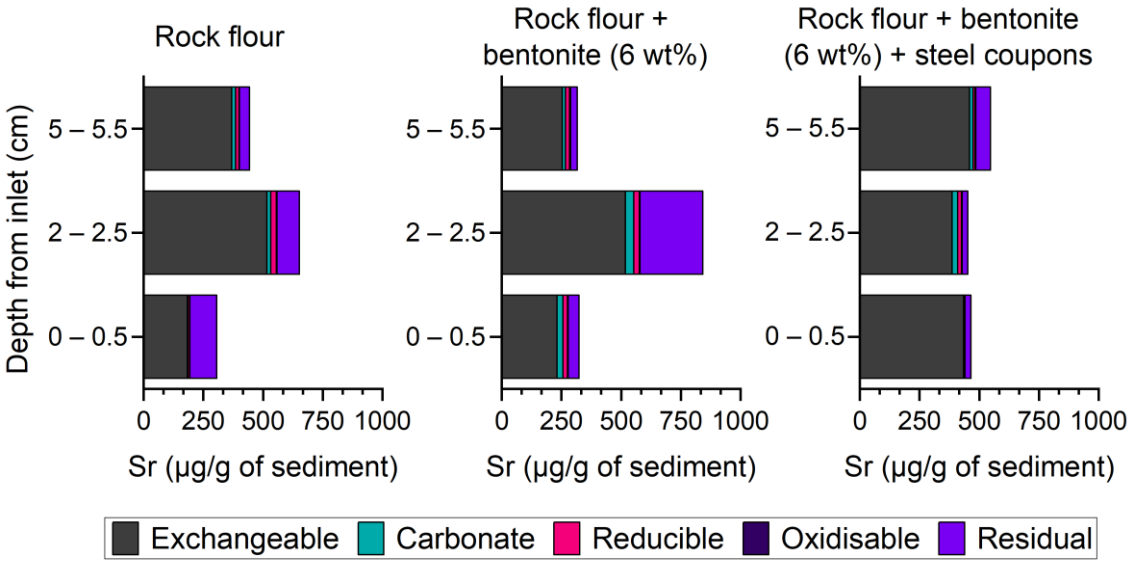

Figure 3. Concentration of Sr extracted per lixiviant (see key) from selected column material samples (0.5 cm depth horizons) from the following: rock flour, rock flour + bentonite (6 wt.%), and rock flour + bentonite (6 wt.%) + steel coupons. Sr that was extractable from the original starting materials (rock flour + bentonite 6 wt.%) was subtracted from the data before plotting (Supplementary Materials Table S2). The repeatability of the extraction was assessed by conducting a triplicate extraction of samples taken from the 0–0.5 cm section of the rock flour column system. Therein, the variability was 2.00%, 0.50%, 0.30%, 0.01%, 0.03%, and 6.00% for Sr extracted from the respective fractions.

3.2.2. Speciation of Solid Phase: XAS

Sr K-edge XAS data were obtained for the top (5.0–5.5 cm) section from each of the three systems. Although the steel coupons were added 1.5 cm away from the column inlet, upon dismantling the columns, a reddish horizon was also observed between 3.0 and 3.5 cm. This was likely due to carbon steel corrosion and some migration of the corrosion products up the column. Therefore, additional XAS data were collected for the 3.0–3.5 cm section from the rock flour + bentonite + carbon steel coupons system to investigate the potential for interactions between the Sr and the corroded steel coupons.

The Sr K-edge XANES data for all samples (Figure S5) were very similar, suggesting a similar local coordination environment of Sr in all these sections, likely with a weakly bound outer-sphere 9-fold oxygen coordination. The background-subtracted EXAFS and their corresponding Fourier transforms are shown in Figure 4 and the accompanying fit parameters are shown in Supplementary Materials Table S4. The best fit of the EXAFS data for the rock flour-only system was with a single shell of 9 O backscatterers at 2.55 Å (Supplementary Materials Table S4), confirming the weak outer-sphere sorption of Sr to a variety of mineral phases [28,31,32,39]. Attempts to fit subsequent shells using sensible parameters (e.g., Fe, Al, Si, and/or C) yielded unsatisfactory fits (unrealistic bond lengths or R-factors >0.02). In all other samples, the EXAFS spectra were best fit with a first backscattering shell containing 9 O backscatterers at 2.54 Å–2.56 Å and a second shell containing 1.4 Si/Al backscatterers at 3.33 Å–3.35 Å (indicated in Figure 4 with an arrow in the Fourier transforms), which statistically improved the fits and is consistent with past Sr sorption onto clays (F-test, 98%–100%, Supplementary Materials Table S4) [31].

Past studies show that Sr sorbs to steel corrosion products (e.g., goethite) as outer-sphere $SrOH^+$ complexes [32,36]. Although EXAFS analysis of the sample indicative of steel corrosion (3.0–3.5 cm section from the rock flour + bentonite (6 wt.%) + steel coupons system) was consistent with outer-sphere sorption, it is impossible to unambiguously define if Sr was interacting with the corroded steel without further analysis (e.g., spatially resolved XAS). Past studies also show that Sr can also precipitate as a strontianite layer

($SrCO_3$) at mineral surfaces [32]. However, unsatisfactory fits when modelling this scenario confirms that strontianite precipitation was not a dominant mechanism for Sr removal.

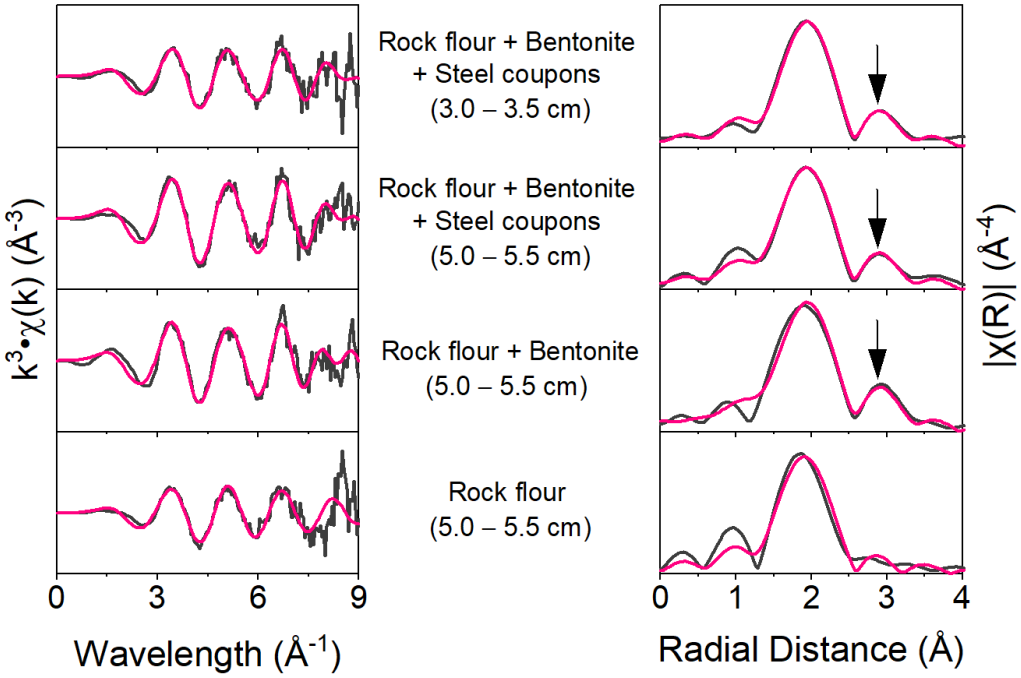

Figure 4. Sr K-edge EXAFS spectra for column material samples and best fits for k^3 weighted data (**left**) and their Fourier transforms (FT) (**right**). Fits are detailed in Supplementary Materials Table S4. Experimental data are shown in black, and best fits (Supplementary Materials Table S4) are in red. The arrow in the Fourier transform indicates the presence of a Si/Al shell.

Interestingly, whilst the sequential extractions indicated the presence of more strongly bound Sr phases (extracted by aqua regia), XAS analysis of select sections from the columns only indicated weak outer-sphere complexes. Clearly some Sr binds to the repository materials in a stronger way (e.g., inner-sphere sorption or coprecipitation), but without completing further XAS analysis (e.g., completing analysis on other column samples or collecting Sr XAS to a higher k), it is not possible to confirm the detail of the stronger Sr retention mechanism(s).

3.3. Remobilisation Experiments

To assess the stability of the Sr associated with the barrier material towards remobilisation, short-term remobilisation experiments using oxic rainwater (28 days) and then oxic seawater (28 days) were run. In both experiments, no Sr was added to the influent solutions.

The influent was changed to artificial rainwater (without added Sr) for the first 28 days of remobilisation experiments. Effluent pH stabilised at ~6.2 in the rock flour and rock-flour + bentonite + steel systems and decreased to ~5.8 in the rock flour + bentonite system (Figure S4). Sr concentrations ranged between 2.4 and 5 mg/L in the effluents of the rock flour rainwater remobilisation system and remained at ≤2.7 mg/L in the other two systems. Interestingly, there was an increase in effluent Sr concentrations in the first sampling point for all three column systems after transition to the Sr-free rainwater. This may reflect physical disturbance of the columns and possible entrainment of Sr-labelled fine-grained material in the effluent. During the transition, the pump was turned off and the influent and effluent lines and columns were handled.

When the influent was changed to seawater, the pH increased marginally to between 6.1 and 6.2 on day 352 (56 days remobilisation) (Figure S4) and effluent Sr concentrations increased (≤40 mg/L) in the systems containing bentonite (6 wt.%) (Figure 5) this was likely

attributable to the increased ionic strength of the seawater, which remobilised significant bentonite-bound Sr, likely via ion-exchange reactions. The rock flour-only system was not significantly affected by the change in influent, suggesting that Sr was bound via a different outer-sphere sorption mechanism, consistent with EXAFS analyses (Figure 5). The effluent Sr concentrations in the bentonite-containing systems remained higher than those observed in the rock flour-only system until the last day (day 352), when both bentonite-containing systems had no Sr in their effluent, suggesting that all weakly bound Sr had left the columns. The increase in Sr mobility in the columns with added bentonite (6 wt.%) is also consistent with the higher cation exchange capacity observed for rock flour + bentonite (6 wt.%) (0.10 meq/g) compared to that of just rock flour (0.07–0.08 meq/g). The potential for colloid formation was assessed following 28 days of remobilisation with rain- and seawater, and similarly, results showed no evidence of colloid formation.

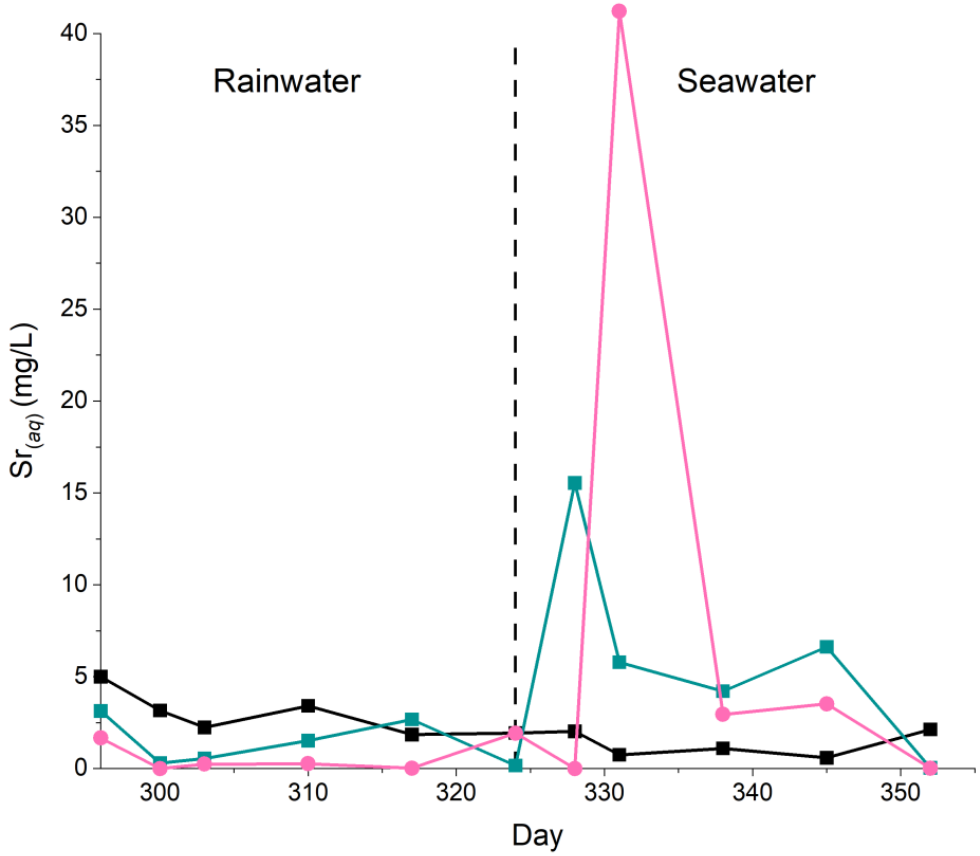

Figure 5. Concentration of $Sr_{(aq)}$ in effluent for three column systems over 56 days of remobilisation experiments: (**black**) rock flour, (**green**) rock flour + bentonite (6 wt.%), and (**pink**) rock flour + bentonite (6 wt.%) + steel coupons, after centrifugation at $1.4 \times 10^4 \times g$ for 5 mins. The dashed line signifies the change from rainwater (left) to seawater (right) input.

4. Conclusions

Flow-through column experiments were used to assess the potential for Sr retention or migration in conditions representative of the Finnish VLLW near-surface repository concept. Three column systems representative of the backfill material placed around the waste packages, mineral sealing layer material, and waste packages were established ((i) rock flour, (ii) rock flour + bentonite (6 wt.%), and (iii) rock flour + bentonite (6 wt.%) + carbon steel coupons) and Sr-labelled synthetic rainwater was pumped through the columns. There was no significant change in the rate or extent of Sr removal from the influent rainwater in the column systems. Moreover, assessments of potential colloid formation at the start and end of the experiment showed no evidence of their presence.

The total Sr retained in the columns, as determined based on aqua regia digests, showed that Sr was evenly distributed throughout the columns and that there was no significant (>20%) difference in total Sr between the different column treatments. Further, Sr was not enriched in the column section where the carbon steel coupons had corroded. Sequential extractions revealed that 68%–87% of Sr associated with the solids was exchangeable with $MgCl_2$, suggesting that the majority of Sr retention occurred via the formation of weakly bound outer-sphere sorption complexes. XAS confirmed that the dominant mechanism for Sr retention was weak outer-sphere sorption, and the addition of Sr-Si/Al backscatterers in the systems containing bentonite (6 wt.%) suggested Sr sorption to bentonites. Significant concentrations of Sr (9%–36%) were also mobilised with aqua regia, indicating that some Sr was more strongly bound. As these Sr phases could not be clearly identified, further investigation into the mechanisms that control Sr retention is merited. Remobilisation experiments found that rainwater was capable of remobilising and transporting Sr through the materials, although perturbations with seawater significantly increased Sr remobilisation in systems containing bentonite (6 wt.%). Sr transport did not change in the rock flour system, suggesting that the Sr–rock flour interactions are stronger than the Sr–bentonite interactions and are therefore less susceptible to ion exchange reactions.

These results demonstrate that the barrier and backfill materials proposed for the Finnish near-surface repository have potential for $Sr_{(aq)}$ removal; however, over the course of the experiments, the sites reactive towards Sr appear to have been largely consumed (an unlikely scenario in the real disposal concept given that the concentrations of Sr used in the current experiments are significantly higher relative to the expected repository conditions). Further, the majority of Sr binding appears to be via a weak interaction. As such, adequate volumes of barrier materials will be needed to limit Sr migration. Protection against issues, such as seawater intrusion, will also be important, to limit the potential for Sr ion exchange. Further study is also needed to define the (potentially useful) stronger Sr binding interaction and also the potential effects of the biodegradation of organic operational wastes. Finally, based on current evidence, corroding waste packages do not appear to significantly complex Sr. Given the relatively small volume of steel used in these experiments, when compared to the corrosion of a fully sized waste canister, we suggest that the effects of steel canister corrosion under similar conditions need to be further studied. These results can feed forward into safety case design for the Finnish near-surface VLLW repository. Moreover, the experimental approach used here offers a stable and facile method for replicating repository environments, which can be easily adapted according to the users' requirements, i.e., studying other risk-driving radionuclides (e.g., ^{137}Cs) or varying backfill materials to simulate other scenarios.

Supplementary Materials: The following supporting information can be downloaded at: https://www.mdpi.com/article/10.3390/min13030436/s1. Figure S1: Main barriers in a landfill-type repository; Figure S2: Schematic of columns; Figure S3: XRD patterns for the rock flour and bentonite; Table S1: Composition of starting materials; Figure S4: pH; Table S2: Concentration of Sr extracted per lixiviant from column starting materials; Table S3: Mass balance of Sr in effluents and Sr associated with column solids in each system; Figure S5: Normalized Sr K-edge XANES spectra; Table S4: EXAFS fit parameters; Table S5 PHREEQC input parameters; Table S6: PHREEQC output. Refs [74–77] are in the supplementary materials.

Author Contributions: Conceptualisation, M.S.H., G.F.V., P.H.K., S.P.L., M.V., E.M. and G.T.W.L.; methodology, M.S.H., G.F.V., K.D. and G.T.W.L.; writing, M.S.H., G.F.V. and G.T.W.L.; review and editing, all; Funding acquisition G.F.V., P.H.K. and G.T.W.L. All authors have read and agreed to the published version of the manuscript.

Funding: Ho acknowledges scholarship funding from the National Research Foundation, Singapore, via the Singapore Nuclear Research and Safety Initiative. Vettese, Law, Keto, Lamminmäki, Myllykylä, and Vikman acknowledge funding from the Finnish KYT programme (project VN/14858/2021). Open access funding provided by University of Helsinki.

Data Availability Statement: The data are available upon request from the corresponding authors.

Acknowledgments: We acknowledge the KIT light source for provision of instruments at the INE beamline operated of the Institute for Nuclear Waste Disposal (INE) at the KIT synchrotron light source and we would like to thank the Institute for Beam Physics and Technology (IBPT) for the operation of the storage ring, the Karlsruhe Research Accelerator (KARA).

Conflicts of Interest: The authors declare no conflict of interest.

References

1. WNA Nuclear Power Today | Nuclear Energy. 2019. Available online: https://www.world-nuclear.org/information-library/current-and-future-generation/nuclear-power-in-the-world-today.aspx (accessed on 31 December 2021).
2. SKB. SFR-Final Repository for Short-Lived Radioactive Waste. 2021. Available online: https://www.skb.com/our-operations/sfr/ (accessed on 22 April 2022).
3. Kumpula, L.; Huhtanen, I.; Palander, S.; Ylä-Mella, M.; Kuhmonen, V. *Management of Spent Nuclear Fuel and Radioactive Waste in Finland*; Ministry of Economic Affairs and Employment Energy: Helsinki, Finland, 2022.
4. IAEA. *Technical Reports Series No.433: Upgrading of Near Surface Repositories for Radioactive Waste*; IAEA: Vienna, Austria, 2005.
5. Tammela, J. Near-Surface Final Disposal. KYT2022 Seminar: Near Surface Disposal in Finland. 3rd of November 2021. 2021. Available online: http://kyt2022.vtt.fi/surface_webinar2021/KYT_2022_KYT_SURFACE_Near_surface_disposal_in_Finland_seminar.pdf (accessed on 6 March 2023).
6. Finlex. *Finlex. Finnish Nuclear Energy Act (990/1987)*; Ministry of Economic Affairs and Employment Energy: Helsinki, Finland, 1987.
7. TVO. *Hyvin Matala-Aktiivisen Jätteen Maaperäloppusijoitus, Olkiluoto [Near-Surface Disposal of Very Low-Level Waste, Olkiluoto]. Environmental Impact Assessment Programme, TVO-11718, 11 August 2020*; TVO: Eurajoki, Finland, 2020.
8. TVO. *Hyvin Matala-Aktiivisen Jätteen Maaperäloppusijoitus, Olkiluoto [Near-Surface Disposal of Very Low-Level Waste, Olkiluoto]. Environmental Impact Assessment Report, TVO-11971, 11 May 2021*; TVO: Eurajoki, Finland, 2021.
9. Byrd, N.; Lloyd, J.R.; Small, J.S.; Taylor, F.; Bagshaw, H.; Boothman, C.; Morris, K. Microbial Degradation of Citric Acid in Low Level Radioactive Waste Disposal: Impact on Biomineralization Reactions. *Front. Microbiol.* **2021**, *12*, 723. [CrossRef] [PubMed]
10. Keto, P.; Gharbieh, H.; Carpén, L.; Ferrera, M.; Somervuori, M.; Rinta-Hiiro, V.; Laikari, A.; Jafari, S.; Vikman, M. KYT SURFACE Near Surface Repositories in Finland. 2020. Available online: http://kyt2022.vtt.fi/raportit_2020/SURFACE_Near%20Surface%20Repositories%20in%20Finland%202019%20vuosiraportti.pdf (accessed on 6 March 2023).
11. NAGRA. *Project Opalinus Clay—Safety Report—Demonstration of Disposal Feasibility for Spent Fuel, Vitrified High Level Waste and Long-Lived Intermediate Level Waste (Entsorgungsnachweis)*; NAGRA: Wettingen, Switzerland, 2003.
12. IAEA. *Near Surface Disposal Facilities for Radioactive Waste: IAEA Safety Standard Series No. SSG-29*; IAEA: Vienna, Austria, 2014; p. 124.
13. LLW Repository Ltd. *The 2011 Environmental Safety Case: Near Field (LLWR/ESC/R(11)10021)*; LLW Repository Ltd.: Cumbria, UK, 2011.
14. Duro, L.; Domènech, C.; Grivé, M.; Roman-Ross, G.; Bruno, J.; Källström, K. Assessment of the Evolution of the Redox Conditions in a Low and Intermediate Level Nuclear Waste Repository (SFR1, Sweden). *Appl. Geochem.* **2014**, *49*, 192–205. [CrossRef]
15. Burke, I.T.; Boothman, C.; Lloyd, J.R.; Livens, F.R.; Charnock, J.M.; McBeth, J.M.; Mortimer, R.J.G.; Morris, K. Reoxidation Behavior of Technetium, Iron, and Sulfur in Estuarine Sediments. *Environ. Sci. Technol.* **2006**, *40*, 3529–3535. [CrossRef]
16. Singleton, M.J.; Woods, K.N.; Conrad, M.E.; DePaolo, D.J.; Dresel, P.E. Tracking Sources of Unsaturated Zone and Groundwater Nitrate Contamination Using Nitrogen and Oxygen Stable Isotopes at the Hanford Site, Washington. *Environ. Sci. Technol.* **2005**, *39*, 3563–3570. [CrossRef]
17. Chorover, J.; Choi, S.; Rotenberg, P.; Serne, R.J.; Rivera, N.; Strepka, C.; Thompson, A.; Mueller, K.T.; O 'day, P.A. Silicon Control of Strontium and Cesium Partitioning in Hydroxide-Weathered Sediments. *Geochim. Et Cosmochim. Acta* **2008**, *72*, 2024–2047. [CrossRef]
18. Gu, B.; Wu, W.M.; Ginder-Vogel, M.A.; Yan, H.; Fields, M.W.; Zhou, J.; Fendorf, S.; Criddle, C.S.; Jardine, P.M. Bioreduction of Uranium in a Contaminated Soil Column. *Environ. Sci. Technol.* **2005**, *39*, 4841–4847. [CrossRef]
19. Saunders, J.A.; Toran, L.E. Modeling of Radionuclide and Heavy Metal Sorption around Low-and High- PH Waste Disposal Sites at Oak Ridge, Tennessee. *Appl. Geochem.* **1995**, *10*, 673–684. [CrossRef]
20. Standring, W.J.F.; Oughton, D.H.; Salbu, B. Potential Remobilization of ^{137}Cs, ^{60}Co, ^{99}Tc, and ^{90}Sr from Contaminated Mayak Sediments in River and Estuary Environments. *Environ. Sci. Technol.* **2002**, *36*, 2330–2337. [CrossRef]
21. Sellafield Ltd. *Monitorning Our Environment—Discharges And Environmental Monitoring—Annual Report 2020*; Sellafield Ltd.: Risley, UK, 2021.
22. Pors Nielsen, S. The Biological Role of Strontium. *Bone* **2004**, *35*, 583–588. [CrossRef]
23. Cleary, A.; Lloyd, J.R.; Newsome, L.; Shaw, S.; Boothman, C.; Boshoff, G.; Atherton, N.; Morris, K. Bioremediation of Strontium and Technetium Contaminated Groundwater Using Glycerol Phosphate. *Chem. Geol.* **2019**, *509*, 213–222. [CrossRef]
24. Thorpe, C.L.; Law, G.T.W.W.; Lloyd, J.R.; Williams, H.A.; Atherton, N.; Morris, K. Quantifying Technetium and Strontium Bioremediation Potential in Flowing Sediment Columns. *Environ. Sci. Technol.* **2017**, *51*, 12104–12113. [CrossRef] [PubMed]

25. Wallace, S.H.; Shaw, S.; Morris, K.; Small, J.S.; Fuller, A.J.; Burke, I.T. Effect of Groundwater PH and Ionic Strength on Strontium Sorption in Aquifer Sediments: Implications for ^{90}Sr Mobility at Contaminated Nuclear Sites. *Appl. Geochem.* **2012**, *27*, 1482–1491. [CrossRef]
26. Trivedi, P.; Axe, L. A Comparison of Strontium Sorption to Hydrous Aluminum, Iron, and Manganese Oxides. *J. Colloid Interface Sci.* **1999**, *218*, 554–563. [CrossRef] [PubMed]
27. Chiang, P.N.; Wang, M.K.; Huang, P.M.; Wang, J.J.; Chiu, C.Y. Cesium and Strontium Sorption by Selected Tropical and Subtropical Soils around Nuclear Facilities. *J. Environ. Radioact.* **2010**, *101*, 472–481. [CrossRef]
28. Axe, L.; Bunker, G.B.; Anderson, P.R.; Tyson, T.A. An XAFS Analysis of Strontium at the Hydrous Ferric Oxide Surface. *J. Colloid Interface Sci.* **1998**, *199*, 44–52. [CrossRef]
29. Balek, V.; Málek, Z.; Šubrt, J.; Ždimera, A. Characterization of Iron(III) Oxide and Oxide-Hydroxide as Sr-Sorbent. *J. Radioanal. Nucl. Chem.* **1996**, *212*, 321–331. [CrossRef]
30. Dyer, A.; Chow, J.; Umar, I.M. The Uptake of Caesium and Strontium Radioisotopes onto Clays. *J. Mater. Chem.* **2000**, *10*, 2734–2740. [CrossRef]
31. Fuller, A.J.; Shaw, S.; Peacock, C.L.; Trivedi, D.; Burke, I.T. EXAFS Study of Sr Sorption to Illite, Goethite, Chlorite, and Mixed Sediment under Hyperalkaline Conditions. *Langmuir* **2016**, *32*, 2937–2946. [CrossRef]
32. Carroll, S.A.; Roberts, S.K.; Criscenti, L.J.; O'day, P.A. Surface Complexation Model for Strontium Sorption to Amorphous Silica and Goethite. *Geochem. Trans.* **2008**, *9*, 2. [CrossRef]
33. Mendez, J.C.; Hiemstra, T. High and Low Affinity Sites of Ferrihydrite for Metal Ion Adsorption: Data and Modeling of the Alkaline-Earth Ions Be, Mg, Ca, Sr, Ba, and Ra. *Geochim. Cosmochim. Acta* **2020**, *286*, 289–305. [CrossRef]
34. García, D.; Lützenkirchen, J.; Huguenel, M.; Calmels, L.; Petrov, V.; Finck, N.; Schild, D. Adsorption of Strontium onto Synthetic Iron(III) Oxide up to High Ionic Strength Systems. *Minerals* **2021**, *11*, 1093. [CrossRef]
35. Lang, A.R.; Engelberg, D.L.; Walther, C.; Weiss, M.; Bosco, H.; Jenkins, A.; Livens, F.R.; Law, G.T.W. Cesium and Strontium Contamination of Nuclear Plant Stainless Steel: Implications for Decommissioning and Waste Minimization. *ACS Omega* **2019**, *4*, 14420–14429. [CrossRef] [PubMed]
36. Sahai, N.; Carroll, S.A.; Roberts, S.; O'day, P.A.; O'day, P.A. X-Ray Absorption Spectroscopy of Strontium(II) Coordination II. Sorption and Precipitation at Kaolinite, Amorphous Silica, and Goethite Surfaces. *J. Colloid Interface Sci.* **2000**, *222*, 198–212. [CrossRef]
37. Hull, L.C.; Schafer, A.L. Accelerated Transport of 90Sr Following a Release of High Ionic Strength Solution in Vadose Zone Sediments. *J. Contam. Hydrol.* **2008**, *97*, 135–157. [CrossRef]
38. Solecki, J. Investigation of ^{85}Sr Adsorption on Selected Soils of Different Horizons. *J. Environ. Radioact.* **2005**, *82*, 303–320. [CrossRef]
39. Chen, C.; Hayes, K.F. X-Ray Absorption Spectroscopy Investigation of Aqueous Co(II) and Sr(II) Sorption at Clay-Water Interfaces. *Geochim. Cosmochim. Acta* **1999**, *63*, 3205–3215. [CrossRef]
40. Khan, S.A.; Riaz-ur-Rehman; Khan, M.A. Sorption of Strontium on Bentonite. *Waste Manag.* **1995**, *15*, 641–650. [CrossRef]
41. Brookshaw, D.R.; Lloyd, J.R.; Vaughan, D.J.; Pattrick, R.A.D. Effects of Microbial Fe(III) Reduction on the Sorption of Cs and Sr on Biotite and Chlorite. *Geomicrobiol. J.* **2016**, *33*, 206–215. [CrossRef]
42. Thorpe, C.L.; Lloyd, J.R.; Law, G.T.W.; Burke, I.T.; Shaw, S.; Bryan, N.D.; Morris, K. Strontium Sorption and Precipitation Behaviour during Bioreduction in Nitrate Impacted Sediments. *Chem. Geol.* **2012**, *306–307*, 114–122. [CrossRef]
43. Thorpe, C.L.; Boothman, C.; Lloyd, J.R.; Law, G.T.W.; Bryan, N.D.; Atherton, N.; Livens, F.R.; Morris, K.; Thorpe, C.L.; Boothman, C.; et al. The Interactions of Strontium and Technetium with Fe(II) Bearing Biominerals: Implications for Bioremediation of Radioactively Contaminated Land. *Appl. Geochem.* **2014**, *40*, 135–143. [CrossRef]
44. Fujita, Y.; Redden, G.D.; Ingram, J.C.; Cortez, M.M.; Ferris, F.G.; Smith, R.W. Strontium Incorporation into Calcite Generated by Bacterial Ureolysis. *Geochim. Cosmochim. Acta* **2004**, *68*, 3261–3270. [CrossRef]
45. Handley-Sidhu, S.; Renshaw, J.C.; Moriyama, S.; Stolpe, B.; Mennan, C.; Bagheriasl, S.; Yong, P.; Stamboulis, A.; Paterson-Beedle, M.; Sasaki, K.; et al. Uptake of Sr^{2+} and Co^{2+} into Biogenic Hydroxyapatite: Implications for Biomineral Ion Exchange Synthesis. *Environ. Sci. Technol.* **2011**, *45*, 6985–6990. [CrossRef]
46. Foster, L.; Morris, K.; Cleary, A.; Bagshaw, H.; Sigee, D.; Pittman, J.K.; Zhang, K.; Vettese, G.; Smith, K.F.; Lloyd, J.R. Biomineralization of Sr by the Cyanobacterium Pseudanabaena Catenata Under Alkaline Conditions. *Front. Earth Sci.* **2020**, *8*, 556244. [CrossRef]
47. Porro, I.; Newman, M.E.; Dunnivant, F.M. Comparison of Batch and Column Methods for Determining Strontium Distribution Coefficients for Unsaturated Transport in Basalt. *Environ. Sci. Technol.* **2000**, *34*, 1679–1686. [CrossRef]
48. Szenknect, S.; Ardois, C.; Dewière, L.; Gaudet, J.P. Effects of Water Content on Reactive Transport of 85Sr in Chernobyl Sand Columns. *J. Contam. Hydrol.* **2008**, *100*, 47–57. [CrossRef] [PubMed]
49. Cao, J.; Bate, B.; Bouazza, A.; Deng, W. Measuring Retardation Factors of Cesium-133 and Strontium-88 Cations Using Column Test. *J. Geotech. Geoenvironmental Eng.* **2019**, *145*, 06019009. [CrossRef]
50. Latrille, C.; Wissocq, A.; Beaucaire, C.; Bildstein, O. Reactive Transport of Strontium in Two Laboratory-Scale Columns: Experiments and Modelling. *J. Contam. Hydrol.* **2021**, *242*, 103850. [CrossRef]

51. Bower, W.R.; Morris, K.; Livens, F.R.; Mosselmans, J.F.W.; Fallon, C.M.; Fuller, A.J.; Natrajan, L.; Boothman, C.; Lloyd, J.R.; Utsunomiya, S.; et al. Metaschoepite Dissolution in Sediment Column Systems—Implications for Uranium Speciation and Transport. *Environ. Sci. Technol.* **2019**, *53*, 9915–9925. [CrossRef]
52. Ho, M.S.; Vettese, G.F.; Morris, K.; Lloyd, J.R.; Boothman, C.; Bower, W.R.; Shaw, S.; Law, G.T.W. Retention of Immobile Se(0) in Flow-through Aquifer Column Systems during Bioreduction and Oxic-Remobilization. *Sci. Total Environ.* **2022**, *834*, 155332. [CrossRef] [PubMed]
53. Forsius, M.; Kleemola, S.; Vuorenmaa, J.; Syri, S. Fluxes and Trends of Nitrogen and Sulphur Compounds at Integrated Monitoring Sites in Europe. *Water. Air. Soil Pollut.* **2001**, *130*, 1641–1648. [CrossRef]
54. Lauttamäki, V.; Kallio, J. Business from Shallow Geothermal Energy Sources: Motives for Using Shallow Geothermal Energy in Various Building Projects [Geoenergiasta Liiketoimintaa: Perusteluja Geoenergian Hyödyntämiselle Erilaisissa Rakennuskohteissa]. *Tutk.—Geol. Tutkimusk.* **2013**, *206*, 72.
55. Lovley, D.R.; Phillips, E.J. Rapid Assay for Microbially Reducible Ferric Iron in Aquatic Sediments. *Appl. Environ. Microbiol.* **1987**, *53*, 1536–1540. [CrossRef] [PubMed]
56. Tessier, A.; Campbell, P.G.C.; Bisson, M. Sequential Extraction Procedure for the Speciation of Particulate Trace Metals. *Anal. Chem.* **1979**, *51*, 844–851. [CrossRef]
57. Keith-Roach, M.J.; Morris, K.; Dahlgaard, H. An Investigation into Technetium Binding in Sediments. *Mar. Chem.* **2003**, *81*, 149–162. [CrossRef]
58. Rothe, J.; Butorin, S.; Dardenne, K.; Denecke, M.A.; Kienzler, B.; Löble, M.; Metz, V.; Seibert, A.; Steppert, M.; Vitova, T.; et al. The INE-Beamline for Actinide Science at ANKA. *Rev. Sci. Instrum.* **2012**, *83*, 43105. [CrossRef]
59. Ravel, B.; Newville, M. ATHENA, ARTEMIS, HEPHAESTUS: Data Analysis for X-Ray Absorption Spectroscopy Using IFEFFIT. *J. Synchrotron Radiat.* **2005**, *12*, 537–541. [CrossRef]
60. Downward, L.; Booth, C.H.; Lukens, W.W.; Bridges, F. A Variation of the F-Test for Determining Statistical Relevance of Particular Parameters in EXAFS Fits. *AIP Conf. Proc.* **2009**, *882*, 129–131. [CrossRef]
61. Yli-Hemminki, P.; Jørgensen, K.S.; Lehtoranta, J. Iron-Manganese Concretions Sustaining Microbial Life in the Baltic Sea: The Structure of the Bacterial Community and Enrichments in Metal-Oxidizing Conditions. *Geomicrobiol. J.* **2014**, *31*, 263–275. [CrossRef]
62. Missana, T.; Alonso, Ú.; Turrero, M.J. Generation and Stability of Bentonite Colloids at the Bentonite/Granite Interface of a Deep Geological Radioactive Waste Repository. *J. Contam. Hydrol.* **2003**, *61*, 17–31. [CrossRef]
63. Missana, T.; Alonso, U.; Albarran, N.; García-Gutiérrez, M.; Cormenzana, J.L. Analysis of Colloids Erosion from the Bentonite Barrier of a High Level Radioactive Waste Repository and Implications in Safety Assessment. *Phys. Chem. Earth Parts A/B/C* **2011**, *36*, 1607–1615. [CrossRef]
64. Bessho, K.; Degueldre, C. Generation and Sedimentation of Colloidal Bentonite Particles in Water. *Appl. Clay Sci.* **2009**, *43*, 253–259. [CrossRef]
65. Huber, F.; Kunze, P.; Geckeis, H.; Schäfer, T. Sorption Reversibility Kinetics in the Ternary System Radionuclide-Bentonite Colloids/Nanoparticles-Granite Fracture Filling Material. *Appl. Geochem.* **2011**, *26*, 2226–2237. [CrossRef]
66. Missana, T.; García-Gutiérrez, M.; Alonso, Ú. Kinetics and Irreversibility of Cesium and Uranium Sorption onto Bentonite Colloids in a Deep Granitic Environment. *Appl. Clay Sci.* **2004**, *26*, 137–150. [CrossRef]
67. Tran, E.L.; Teutsch, N.; Klein-BenDavid, O.; Weisbrod, N. Uranium and Cesium Sorption to Bentonite Colloids under Carbonate-Rich Environments: Implications for Radionuclide Transport. *Sci. Total Environ.* **2018**, *643*, 260–269. [CrossRef] [PubMed]
68. Albarran, N.; Missana, T.; García-Gutiérrez, M.; Alonso, U.; Mingarro, M. Strontium Migration in a Crystalline Medium: Effects of the Presence of Bentonite Colloids. *J. Contam. Hydrol.* **2011**, *122*, 76–85. [CrossRef]
69. García-García, S.; Wold, S.; Jonsson, M. Effects of Temperature on the Stability of Colloidal Montmorillonite Particles at Different PH and Ionic Strength. *Appl. Clay Sci.* **2009**, *43*, 21–26. [CrossRef]
70. García-García, S.; Degueldre, C.; Wold, S.; Frick, S. Determining Pseudo-Equilibrium of Montmorillonite Colloids in Generation and Sedimentation Experiments as a Function of Ionic Strength, Cationic Form, and Elevation. *J. Colloid Interface Sci.* **2009**, *335*, 54–61. [CrossRef] [PubMed]
71. Zhang, Q.; Zheng, M.; Huang, Y.; Kunte, H.J.; Wang, X.; Liu, Y.; Zheng, C. Long Term Corrosion Estimation of Carbon Steel, Titanium and Its Alloy in Backfill Material of Compacted Bentonite for Nuclear Waste Repository. *Sci. Rep.* **2019**, *9*, 3195. [CrossRef]
72. Rajala, P.; Carpén, L.; Vepsäläinen, M.; Raulio, M.; Sohlberg, E.; Bomberg, M. Microbially Induced Corrosion of Carbon Steel in Deep Groundwater Environment. *Front. Microbiol.* **2015**, *6*, 647. [CrossRef] [PubMed]
73. Gerke, T.L.; Little, B.J.; Luxton, T.P.; Scheckel, K.G.; Maynard, J.B. Strontium Concentrations in Corrosion Products from Residential Drinking Water Distribution Systems. *Environ. Sci. Technol.* **2013**, *47*, 5171–5177. [CrossRef]
74. SYKE. *Kaatopaikan Tiivistysrakenteet. Ymparistoopas 36*; SYKE: Helsinki, Finland, 2002; ISBN 952-11-0232-2.
75. SYKE. *Kaatopaikkojen Kaytosta Poistaminen Ja Jalkihoito. Ymparistohallinnon Ohjeita 1/2008*; SYKE: Helsinki, Finland, 2008; ISBN 978-952-11-3151-6.

76. IAEA. *Scientific and Technical Basis for the Near Surface Disposal of Low and Intermediate Level Waste: Scientific and Technical Basis for the Near Surface Disposal of Low and Intermediate Level Waste*; IAEA: Vienna, Austria, 2002.
77. Posiva Oy. *Measurements on Cation Exchange Capacity of Bentonite in the Long-Term Test of Buffer Material (LOT)*; No POSIVA-WR-11-10; POSIVA: Eurajoki, Finland, 2011.